Model Predictive Based Unscented Kalman Filter for Hypersonic Vehicle Navigation With INS/GNSS Integration

GAOGE HU[1], **LONGQIANG NI**[2], **BINGBING GAO**[1], **XINHE ZHU**[3], **WEI WANG**[4], **AND YONGMIN ZHONG**[3]

[1]School of Automation, Northwestern Polytechnical University, Xi'an 710072, China
[2]Northwest Institute of Mechanical and Engineering, Xianyang 712099, China
[3]School of Engineering, RMIT University, Bundoora, VIC 3083, Australia
[4]CRRC Yongji Electric Company, Xi'an 710018, China

Corresponding author: Bingbing Gao (nwpugbb0826@126.com)

ABSTRACT The INS/GNSS integration is the commonly used technique for hypersonic vehicle navigation. However, owing to the complicated flight dynamics with high maneuverability and large flight envelope, the dynamic model of INS/GNSS integration inevitably exists errors which degrades the navigation performance of a hypersonic vehicle seriously. In this paper, a new model predictive based unscented Kalman filter (MP-UKF) is proposed to address this problem. The MP-UKF employs the concept of model predictive filter for the establishment of a dynamic model error estimator, and it subsequently compensate the model error estimation to UKF for nonlinear state estimation. Since the MP-UKF could predict the dynamic model error persistently and correct the filtering procedure of UKF online, it improves the UKF adaptiveness and is promising for the performance enhancement of INS/GNSS integration for hypersonic vehicle navigation. Simulation results and comparison analysis have been conducted to demonstrate the effectiveness of the proposed method.

INDEX TERMS Unscented Kalman filter, model predictive filter, hypersonic vehicle navigation, INS/GNSS integration, dynamic model error.

I. INTRODUCTION

Hypersonic vehicle, which is a kind of vehicles at the speed of Mach 5 or above, provides a cost-effective way to access space by reducing the flight time. It has received significantly resurgent interests in recent years since the two successful flight tests of the X-43A conducted by national aeronautics and space administration (NASA) [1], [2]. As one of the key technologies of hypersonic vehicle, precise navigation technique is essential for ensuring the feasibility and efficiency of hypersonic vehicle. However, achieving precise navigation information for the hypersonic vehicle is still a challenging task, which is caused by the high maneuverability and large flight envelope [3]–[6].

The associate editor coordinating the review of this manuscript and approving it for publication was Venkata Ratnam Devanaboyina.

Nowadays, the most commonly used and representative navigation system for hypersonic vehicles is the INS/GNSS (inertial navigation system/global navigation satellite system) integration [5]. This integrated navigation system allows to completely exploits the individual advantages of INS and GNSS, such as the consistently high-accuracy trajectory information of GNSS and the short term stability of INS, which make the optimistic solution to enhance the navigation accuracy a reality [5]–[8]. In fact, the INS/GNSS integration system has been adopted by NASA in a series of hypersonic vehicles, such as X-43A, X-51A and HTV-2 [1], [9].

State estimation is of importance for the navigation solution of hypersonic vehicles. For a linear model, Kalman filtering (KF) is optimal under minimum mean square error criterion and an effective tool for state estimation. However, the INS/GNSS integration system is usually nonlinear in essence [10], [11]. In some cases with a particular focus on

real-time computational performance, the nonlinear system of INS/GNSS integration can be linearized by neglecting nonlinear items under certain assumptions in order to reduce the computational load. However, in most practical applications especially for the hypersonic vehicle, as it is difficult to satisfy these assumptions due to the high maneuverability and large flight envelope, the nonlinear system model should be employed by INS/GNSS integration to describe the complete propagation process of system error and reflect the real system characteristics. As a result, a nonlinear filtering method is required to preferably fuse the navigation information from INS and GNSS [10]–[12].

The extended Kalman filter (EKF) is the typically used nonlinear filtering method for INS/GNSS integration. It linearizes the nonlinear system model via first-order Taylor series expansion so that the linear Kalman filter can be applied [13]. However, for systems with a high degree of nonlinearity, the linearization will cause large truncation error which make EKF output unstable filtering solution. In light of the intuition that to approximate a probability distribution is easier than to approximate an arbitrary nonlinear transformation, the deterministic sampling based unscented Kalman filter (UKF) is proposed as an improvement to EKF. It has been demonstrated in many literatures that UKF is generally superior to EKF in terms of accuracy, and the computational complexities of the two algorithms are roughly in the same order [14]–[16]. However, similar to EKF, the implementation of UKF requires that the system models are pre-defined exactly. If the models involve errors, the UKF estimation will be deteriorated [17]. As to the INS/GNSS integration system for hypersonic vehicle navigation, owning to the complicated flight dynamics with high maneuverability and large flight envelope, it is scarcely possible to establish the vehicle's dynamic model accurately [18], [19]. Whereas the exquisite measurement model can be obtained based on the prior physical characteristics of measurement device and its precision could be improved furtherly using a large amount of available measurement data [10]. As a result, the performance of INS/GNSS integration for hypersonic vehicle navigation is mainly subject to the inherent errors in dynamic model, and it is required that the employed nonlinear filtering algorithms for navigation parameters resolution should have the capability to handle the dynamic model errors.

To enhance the estimation performance of UKF in presence of dynamic model errors, various adaptive methods have been reported. Soken and Hajiyev studied an adaptive fading UKF (AFUKF) by introducing a scale factor to adjust the Kalman filer gain [20]. However, since the scale factor is determined empirically, it may lead to a suboptimal or biased filtering solution. Cho and Choi developed a sigma-point based receding horizon Kalman filter (SPRHKF) to improve the UKF adaptiveness against dynamic model error and temporarily unknown sensor bias [21]. However, since this filter is based on a finite impulse response structure, its convergence is poor. Based on the covariance matching technique, Meng et al. reported an adaptive UKF by estimating

and adjusting the noise covariance online to compensate the model uncertainty [22]. However, the use of the covariance matching yields a steady-state estimation error, leading to a limited improvement in the filtering accuracy. Song and Han presented an adaptive method to update the covariance of process noise by minimizing the difference between the computed and actual innovation covariances [23]. However, this filter requires the calculation of partial derivatives, leading to a large computational load.

The model predictive filter (MPF) provides a solution to determine the dynamic model for the optimal state estimation. The MPF estimates the dynamic model error by comparing the filtering outputs with the actual measurements, and subsequently correct the dynamic model in the filtering procedure based on the determined model error to obtain a preferable system state estimation [24], [25]. Due to the real-time performance in state estimation and the correction of dynamic model, the MPF is capable to achieve superior filtering performance in presence of dynamic model error in comparison with EKF and UKF [26]. However, the imperfection of MPF lies in its low convergence rate [27]. Thus it is promising to combine the MPF with UKF to overcome their respective limitations. Nevertheless, there has been very limited research focusing on using the concept of MPF to improve the UKF adaptiveness.

This paper presents a novel model predictive based unscented Kalman filter (MP-UKF) for hypersonic vehicles navigation with INS/GNSS integration. The MP-UKF employs the concept of model predictive filter to establish an estimator for the prediction of dynamic model error, and then it compensates the model error estimation to the UKF procedure for nonlinear state estimation. The proposed MP-UKF enables to correct the UKF sensitivity to dynamic model error persistently, thus it overcomes the limitation of UKF and is promising for hypersonic vehicle navigation. Simulations and comparison analysis with the UKF and AFUKF have been conducted to comprehensively verify the effectiveness and superiority of the proposed MP-UKF.

II. MATHEMATICAL MODEL OF INS/GNSS INTEGRATION FOR HYPERSONIC VEHICLES

The INS and GNSS are integrated to generate navigation solution for hypersonic vehicles by using the high-precision GNSS position and velocity to correct the INS velocity and position errors. In INS/GNSS integration, the dynamic model is constructed by combining the INS error equation with the inertial measurement unit (IMU) error equation, and the measurement model is established based on the difference between INS and GNSS in terms of velocity and position.

A. DYNAMIC MODEL

The local navigation frame (n-frame) is selected as the East-North-Up (E-N-U) geography frame. Denote the inertial frame by i, the earth frame by e, the body frame by b and the INS simulated platform frame by n'. The attitude and velocity

error equations with large initial error is formulated as [12].

$$
\begin{cases}
\dot{\boldsymbol{\phi}} = \boldsymbol{C}_\omega^{-1}[(\boldsymbol{I} - \boldsymbol{C}_n^{n'})\hat{\boldsymbol{\omega}}_{in}^n + \boldsymbol{C}_n^{n'}\delta\boldsymbol{\omega}_{in}^n - \boldsymbol{C}_b^{n'}\delta\boldsymbol{\omega}_{ib}^b] \\
\delta\dot{\boldsymbol{v}}^n = [\boldsymbol{I} - (\boldsymbol{C}_n^{n'})^{\mathrm{T}}]\boldsymbol{C}_b^{n'}\hat{\boldsymbol{f}}^b + \boldsymbol{C}_b^n\delta\boldsymbol{f}^b \\
\quad - (2\hat{\boldsymbol{\omega}}_{ie}^n + \hat{\boldsymbol{\omega}}_{en}^n) \times \delta\boldsymbol{v}^n \\
\quad - (2\delta\boldsymbol{\omega}_{ie}^n + \delta\boldsymbol{\omega}_{en}^n) \times \boldsymbol{v}^n
\end{cases} \tag{1}
$$

where $\boldsymbol{\phi} = (\phi_E, \phi_N, \phi_U)^{\mathrm{T}}$ and $\delta\boldsymbol{v}^n = (\delta v_E, \delta v_U, \delta v_N)^{\mathrm{T}}$ are the attitude and velocity errors solved in n-frame; $\boldsymbol{v}^n = (v_E, v_U, v_N)^{\mathrm{T}}$ is the velocity of the vehicle; $\boldsymbol{C}_n^{n'}$, $\boldsymbol{C}_b^{n'}$ and $\boldsymbol{C}_b^n$ are the rotation matrices; $\hat{\boldsymbol{f}}^b$ is the measured specific force in b-frame, which is composed of accelerometer zero-bias ∇^b and white noise $\boldsymbol{\omega}_a^b$, $\delta\boldsymbol{f}^b$ is the corresponding error vector; $\delta\boldsymbol{\omega}_{ib}^b$ is the measurement error of gyro, which is composed of gyro constant drift $\boldsymbol{\varepsilon}^b$ and white noise $\boldsymbol{\omega}_g^b$; $\boldsymbol{\omega}_{ie}^n$ is the rotational angular velocity of the earth, $\boldsymbol{\omega}_{en}^n$ is the angular velocity of the vehicle relative to the earth, $\boldsymbol{\omega}_{in}^n = \boldsymbol{\omega}_{ie}^n + \boldsymbol{\omega}_{en}^n$ is the relative angular velocity between the n-frame and i-frame, $\hat{\boldsymbol{\omega}}_{ie}^n$, $\hat{\boldsymbol{\omega}}_{en}^n$ and $\hat{\boldsymbol{\omega}}_{in}^n$ are the values of $\boldsymbol{\omega}_{ie}^n$, $\boldsymbol{\omega}_{en}^n$ and $\boldsymbol{\omega}_{in}^n$ solved in n'-frame, $\delta\boldsymbol{\omega}_{ie}^n$, $\delta\boldsymbol{\omega}_{en}^n$ and $\delta\boldsymbol{\omega}_{in}^n$ represent the corresponding errors; $\boldsymbol{C}_\omega^{-1}$ is a relation matrix transforming the relative angular velocity between n'-frame and n-frame into the Euler angle error, which can be computed as

$$
\boldsymbol{C}_\omega^{-1} = \frac{1}{\cos\phi_E}
$$
$$
\times \begin{bmatrix}
\cos\phi_N\cos\phi_E & 0 & \sin\phi_N\cos\phi_E \\
\sin\phi_N\sin\phi_E & \cos\phi_E & -\cos\phi_N\sin\phi_E \\
-\sin\phi_N & 0 & \cos\phi_N
\end{bmatrix} \tag{2}
$$

The position error equation of INS is given by

$$
\begin{cases}
\delta\dot{L} = \dfrac{\delta v_N}{R_M + h} - \delta h\dfrac{v_N}{(R_M + h)^2} \\
\delta\dot{\lambda} = \dfrac{\delta v_E\sec L}{R_N + h} + \delta L\dfrac{v_E\tan L\sec L}{R_N + h} - \delta h\dfrac{v_E\sec L}{(R_N + h)^2} \\
\delta\dot{h} = \delta v_U
\end{cases} \tag{3}
$$

where L and h are the latitude and altitude of the hypersonic vehicle; R_M and R_N are the median radius and normal radius, respectively.

As to the gyro constant drift $\boldsymbol{\varepsilon}^b$ and accelerometer zero-bias ∇^b, they are commonly expressed as random constants: i.e.

$$
\dot{\boldsymbol{\varepsilon}}_i^b = 0 \quad (i = x, y, z) \tag{4}
$$
$$
\dot{\nabla}_i^b = 0 \quad (i = x, y, z) \tag{5}
$$

We define the system state vector as:

$$
\boldsymbol{x}(t) = [\phi_E, \phi_N, \phi_U, \delta v_E, \delta v_N, \delta v_U, \delta L, \delta\lambda, \delta h,
$$
$$
\varepsilon_x^b, \varepsilon_y^b, \varepsilon_z^b, \nabla_x^b, \nabla_y^b, \nabla_z^b]^{\mathrm{T}} \tag{6}
$$

Then the dynamic model of INS/GNSS integration for hypersonic vehicles can be established by combining equations (1)-(5)

$$
\dot{\boldsymbol{x}}(t) = \bar{f}(\boldsymbol{x}(t)) + \boldsymbol{w}(t) \tag{7}
$$

where $\bar{f}(\cdot)$ is a nonlinear function describing the aforementioned INS error equation IMU error equation in continuous form; and $\boldsymbol{w}(t) = \left[\left(-\boldsymbol{C}_\omega^{-1}\boldsymbol{C}_b^{n'}\boldsymbol{\omega}_a^b\right)^{\mathrm{T}}, \left(\boldsymbol{C}_b^n\boldsymbol{\omega}_g^b\right)^{\mathrm{T}}, \boldsymbol{0}_{1\times9}\right]^{\mathrm{T}}$ is the process noise vector.

Discretizing (7) by use of the improved Euler formulation presented in [28], the dynamic model of INS/GNSS integration in discrete-time form can be expressed as

$$
\boldsymbol{x}_k = f(\boldsymbol{x}_{k-1}) + \boldsymbol{w}_k \tag{8}
$$

where $f(\cdot)$ is a discretized nonlinear function describing the dynamics of system state; and $\boldsymbol{w}(k)$ is the discrete-time process noise.

B. MEASUREMENT MODEL

Denote the velocity and position solved by INS as $(v_{EI}, v_{NI}, v_{UI})^{\mathrm{T}}$ and $(L_I, \lambda_I, h_I)^{\mathrm{T}}$; the corresponding outputs from GNSS as $(v_{EG}, v_{NG}, v_{UG})^{\mathrm{T}}$ and $(L_G, \lambda_G, h_G)^{\mathrm{T}}$. We take the difference between INS and GNSS in terms of velocity and position as measurement vector, i.e. (9), as shown at the bottom of the next page.

Then the measurement model of INS/GNSS integration for hypersonic vehicle navigation can be established by

$$
\boldsymbol{z}_k = \boldsymbol{H}_k\boldsymbol{x}_k + \boldsymbol{v}_k = \begin{bmatrix} \boldsymbol{H}_{v,k} \\ \boldsymbol{H}_{p,k} \end{bmatrix}\boldsymbol{x}_k + \begin{bmatrix} \boldsymbol{v}_{v,k} \\ \boldsymbol{v}_{p,k} \end{bmatrix} \tag{10}
$$

where $\boldsymbol{H}_{p,k} = [\boldsymbol{0}_{3\times6}, diag(R_M, R_N\cos L, 1), \boldsymbol{0}_{3\times6}]$ and $\boldsymbol{H}_{v,k} = [\boldsymbol{0}_{3\times3}, \boldsymbol{I}_{3\times3}, \boldsymbol{0}_{3\times9}]$; $\boldsymbol{v}_{v,k}$ and $\boldsymbol{v}_{p,k}$ are the measurement noises corresponding to the velocity and position errors of GNSS receiver.

III. MODEL PREDICTIVE BASED UNSCENTED KALMAN FILTER

In this section, the new MP-UKF is derived rigorously for nonlinear state estimation in presence of dynamic model error.

A. CLASSICAL UNSCENTED KALMAN FILTER

To demonstrate the derivation of MP-UKF clearly, the classical UKF is briefly reviewed at first. Consider the nonlinear stochastic system consisting of (8) and (10)

$$
\begin{cases}
\boldsymbol{x}_k = f(\boldsymbol{x}_{k-1}) + \boldsymbol{w}_k \\
\boldsymbol{z}_k = \boldsymbol{H}_k\boldsymbol{x}_k + \boldsymbol{v}_k
\end{cases} \tag{11}
$$

where $\boldsymbol{x}_k \in \mathbf{R}^n$ and $\boldsymbol{z}_k \in \mathbf{R}^m$ are the state and measurement vector at time k; $\boldsymbol{w}_k \in \mathbf{R}^n$ and $\boldsymbol{v}_k \in \mathbf{R}^m$ are additive Gaussian white noise with zeros mean vectors and covariance matrices $\boldsymbol{Q}_k$ and $\boldsymbol{R}_k$; $f(\cdot)$ is the nonlinear function describing the dynamic model and $\boldsymbol{H}_k \in \mathbf{R}^{m\times n}$ is the measurement matrix.

The procedure to implement the classical UKF for the nonlinear system given by (11) is summarized as follows:

Step 1 (Initialization): Initialize the state estimate $\hat{\boldsymbol{x}}_0$ and its error covariance $\hat{\boldsymbol{P}}_0$ with

$$
\begin{cases}
\hat{\boldsymbol{x}}_0 = E[\boldsymbol{x}_0] \\
\boldsymbol{P}_0 = E[(\boldsymbol{x}_0 - \hat{\boldsymbol{x}}_0)(\boldsymbol{x}_0 - \hat{\boldsymbol{x}}_0)^{\mathrm{T}}]
\end{cases} \tag{12}
$$

Step 2 (Time Update): Given the state estimate $\hat{x}_{k-1}$ and the error covariance matrix $\hat{P}_{k-1}$, select the sigma points by

$$\begin{cases} \boldsymbol{\chi}_{i,k-1} = \hat{x}_{k-1}, \\ \qquad i = 0 \\ \boldsymbol{\chi}_{i,k-1} = \hat{x}_{k-1} + \left(a\sqrt{n\hat{P}_{k-1}} \right)_i, \\ \qquad i = 1, 2, \cdots, n \\ \boldsymbol{\chi}_{i,k-1} = \hat{x}_{k-1} - \left(a\sqrt{n\hat{P}_{k-1}} \right)_{i-n}, \\ \qquad i = n+1, n+2, \cdots, 2n \end{cases} \quad (13)$$

where a determines the spread of the sigma points around $\hat{x}_{k-1}$ and is usually set to a small positive value, and $\left(\sqrt{n\hat{P}_{k-1}} \right)_i$ denotes the ith column of the square root of the matrix $n\hat{P}_{k-1}$.

These sigma points are instantiated through the dynamic model to yield a set of transformed samples

$$\boldsymbol{\chi}_{i,k/k-1} = f(\boldsymbol{\chi}_{i,k-1}), \quad i = 0, 1, \cdots, 2n \quad (14)$$

The predicted state mean and covariance are computed as

$$\hat{x}_{k/k-1} = \sum_{i=0}^{2n} \omega_i \boldsymbol{\chi}_{i,k/k-1} = \sum_{i=0}^{2n} \omega_i f(\boldsymbol{\chi}_{i,k-1}) \quad (15)$$

$$\hat{P}_{k/k-1} = \sum_{i=0}^{2n} \omega_i (\boldsymbol{\chi}_{i,k/k-1} - \hat{x}_{k/k-1})(\boldsymbol{\chi}_{i,k/k-1} - \hat{x}_{k/k-1})^{\mathrm{T}} + \boldsymbol{Q}_k \quad (16)$$

where $\begin{cases} \omega_i = 1 - \frac{1}{a^2}, & i = 0 \\ \omega_i = \frac{1}{2na^2}, & i = 1, 2, \cdots, 2n \end{cases}$.

Step 3 (Measurement Update): Since the measurement model is in a linear form, the update process can be performed in the same way as the Kalman filter, i.e.

$$\hat{z}_{k/k-1} = \boldsymbol{H}_k \hat{x}_{k/k-1} \quad (17)$$

$$\hat{P}_{\hat{z}_{k/k-1}} = \boldsymbol{H}_k \hat{P}_{k/k-1} \boldsymbol{H}_k^{\mathrm{T}} + \boldsymbol{R}_k \quad (18)$$

$$\hat{P}_{\hat{x}_{k/k-1}\hat{z}_{k/k-1}} = \hat{P}_{k/k-1} \boldsymbol{H}_k^{\mathrm{T}} \quad (19)$$

$$\boldsymbol{K}_k = \hat{P}_{\hat{x}_{k/k-1}\hat{z}_{k/k-1}} \hat{P}_{\hat{z}_{k/k-1}}^{-1} \quad (20)$$

$$\hat{x}_k = \hat{x}_{k/k-1} + \boldsymbol{K}_k(z_k - \hat{z}_{k/k-1}) \quad (21)$$

$$\hat{P}_k = \hat{P}_{k/k-1} - \boldsymbol{K}_k \hat{P}_{\hat{z}_{k/k-1}} \boldsymbol{K}_k^{\mathrm{T}} \quad (22)$$

Step 4: Repeat Steps 2 to 3 for the next time step.

It can be seen from the implementation procedure of the classical UKF that if the system model involves the dynamic model error, the predicted state $\hat{x}_{k/k-1}$ will become inaccurate. Further, it will make the Kalman gain $\boldsymbol{K}_k$ biased, deteriorating the state estimate obtained from (21). Therefore, without the compensatation of dynamic model error, the filtering solution of the classical UKF will be unreliable or even divergent.

B. MPF BASED DYNAMIC MODEL ERROR ESTIMATION

The MPF can effectively solve the state estimation problem of nonlinear system with any form of dynamic model error. It is proposed based on a continuous nonlinear system, which is described as

$$\dot{x}(t) = f(x(t)) + G(t)\boldsymbol{d}(t) \quad (23)$$

$$z(t) = h(x(t)) + v(t) \quad (24)$$

where $x(t) \in \boldsymbol{R}^n$ is the state vector; $f(\cdot)$ is the differentiable model function; $G(t) \in \boldsymbol{R}^{n \times l}$ is the model error distribution matrix; $\boldsymbol{d}(t) \in \boldsymbol{R}^l$ is the model error vector; $h(x(t))$ is the measurement function, $z(t) \in \boldsymbol{R}^m$ is the measurement vector, and $v(t) \in \boldsymbol{R}^m$ is the measurement noise which obeys Gaussian white-noise distributed process with covariance $\boldsymbol{R}$.

From the nonlinear system (23) and (24), the state and output estimates can be given by

$$\dot{\hat{x}}(t) = f(\hat{x}(t)) + G(t)\boldsymbol{d}(t) \quad (25)$$

$$\hat{z}(t) = h(\hat{x}(t)) \quad (26)$$

Expanding the output estimate in (26) by a Taylor series, we have

$$\hat{z}(t + \Delta t) \approx \hat{z}(t) + S(\hat{x}(t), \Delta t) + \Lambda(\Delta t)U(\hat{x}(t))\boldsymbol{d}(t) \quad (27)$$

where $\Lambda(\Delta t) \in \boldsymbol{R}^{m \times m}$ is a diagonal matrix with elements given by

$$\lambda_{ii} = \frac{\Delta t^{p_i}}{p_i!}, \quad i = 1, 2, \cdots, m \quad (28)$$

$U(\hat{x}(t)) \in \boldsymbol{R}^{m \times l}$ is a matrix with the ith row

$$U_i(\hat{x}(t)) = \left[L_{g1} L_f^{p_i - 1}(h_i), \cdots, L_{gl} L_f^{p_i - 1}(h_i) \right] \quad i = 1, 2, \cdots, m \quad (29)$$

and $S(\hat{x}(t), \Delta t) \in \boldsymbol{R}^m$ is a vector with the ith element

$$S_i(\hat{x}(t), \Delta t) = \sum_{k=1}^{p_i} \frac{\Delta t^k}{k!} L_f^k(h_i) \quad (30)$$

where $p_i(i = 1, 2, \cdots, m)$ is the lowest order of the derivative of $h_i(\hat{x}(t))$ in which any component of $\boldsymbol{d}(t)$ appeared for the first time in $\hat{x}(t)$, and $L_f^k(h_i)$ is the kth-order Lie derivative [24].

The core problem of MPF is to estimate the dynamic model error $\boldsymbol{d}(t)$ by minimizing the cost functional defined as follows

$$J(\boldsymbol{d}(t)) = \frac{1}{2} \left[z(t + \Delta t) - \hat{z}(t + \Delta t) \right]^{\mathrm{T}} \boldsymbol{R}^{-1} \left[z(t + \Delta t) - \hat{z}(t + \Delta t) \right] + \frac{1}{2} \boldsymbol{d}^{\mathrm{T}}(t) \boldsymbol{W} \boldsymbol{d}(t) \quad (31)$$

where $\boldsymbol{W} \in \boldsymbol{R}^{l \times l}$ is the positive semi-definite weighting matrix for model error.

$$z_k = \begin{bmatrix} v_{EI} - v_{EG} & v_{NI} - v_{NG} & v_{UI} - v_{UG} & L_I - L_G & \lambda_I - \lambda_G & h_I - h_G \end{bmatrix}^{\mathrm{T}} \quad (9)$$

Substituting (27) in to (31) and minimizing (31) with respect to $d(t)$, the following model error solution can be obtained:

$$\hat{d}(t) = - \left\{ [\mathbf{\Lambda}(\Delta t)\mathbf{U}(\hat{x}(t))]^{\mathrm{T}} \mathbf{R}^{-1} [\mathbf{\Lambda}(\Delta t)\mathbf{U}(\hat{x}(t))] + \mathbf{W} \right\}^{-1}$$
$$\times [\mathbf{\Lambda}(\Delta t)\mathbf{U}(\hat{x}(t))]^{\mathrm{T}} \mathbf{R}^{-1} [\mathbf{S}(\hat{x}(t), \Delta t) - z(t+\Delta t) + \hat{z}(t)] \tag{32}$$

Since INS/GNSS integration is a discrete-time system in practical application, we assume that the sampling rate is a constant such that $z(t_k) \equiv z_k$ and $z(t_k + \Delta t) \equiv z_{k+1}$. Then the MPF based dynamic model error estimator in discrete form can be yielded from (32), which is given by

$$\hat{d}_k = - \left\{ [\mathbf{\Lambda}(\Delta t)\mathbf{U}(\hat{x}_k)]^{\mathrm{T}} \mathbf{R}^{-1} [\mathbf{\Lambda}(\Delta t)\mathbf{U}(\hat{x}_k)] + \mathbf{W} \right\}^{-1}$$
$$\times [\mathbf{\Lambda}(\Delta t)\mathbf{U}(\hat{x}_k)]^{\mathrm{T}} \mathbf{R}^{-1} [\mathbf{S}(\hat{x}_k, \Delta t) - z_{k+1} + \hat{z}_k] \tag{33}$$

It should be noted that in the proposed MP-UKF, the measurement z_{k+1} in time step t_{k+1} is processed in (33) to compute the model error $\hat{d}_k$ in time segment $[t_k, t_{k+1}]$, and the obtained estimate is subsequently compensated to the nonlinear system (11) for nonlinear state estimaton and furtherly improve the UKF adaptiveness.

Remark 1: The weighting matrix $\mathbf{W}$ in (31) serves to control the amount of model error used for correcting the assumed model (23). As $\mathbf{W}$ decreases, more model error is added to correct the model, so that the state estimation follows the measurements more closely. As $\mathbf{W}$ increases, less model error is added, so that the estimation follow the dynamic model more closely. It is notable that the weighting matrix $\mathbf{W}$ can be determined adaptively based on the covariance constraint condition presented in [24].

Remark 2: In the application of (33) for hypersonic vehicle navigation, the sampling period Δt can be determined according to the discretization period used in (8).

C. MP-UKF ALGORITHM

Based on concept of MPF, the proposed MP-UKF has the capability to estimate the dynamic model error persistently and correct the filtering procedure of UKF online. The flowchart of MP-UKF is shown in Fig. 1, and the implementing process for the proposed method can be summarized as follows.

Step 1: Suppose the state estimate $\hat{x}_k$ and the error covariance matrix $\hat{P}_k$ are given, the output estimate of the system presented by (11) can be calculated as

$$\hat{z}_k = \mathbf{H}_k \hat{x}_k \tag{34}$$

Step 2: Denote the sampling period as Δt. According to (28)-(30), the parameters $\mathbf{\Lambda}(\Delta t)$, $\mathbf{U}(\hat{x}(t))$ and $\mathbf{S}(\hat{x}(t), \Delta t)$ can be computed based on MPF. Thus, the model error estimate $\hat{d}_k$ for the time interval $[t_k, t_{k+1}]$ is obtained from (33).

Step 3: Perform the UKF prediction and use the estimate of dynamic model error to correct the predicted system state,
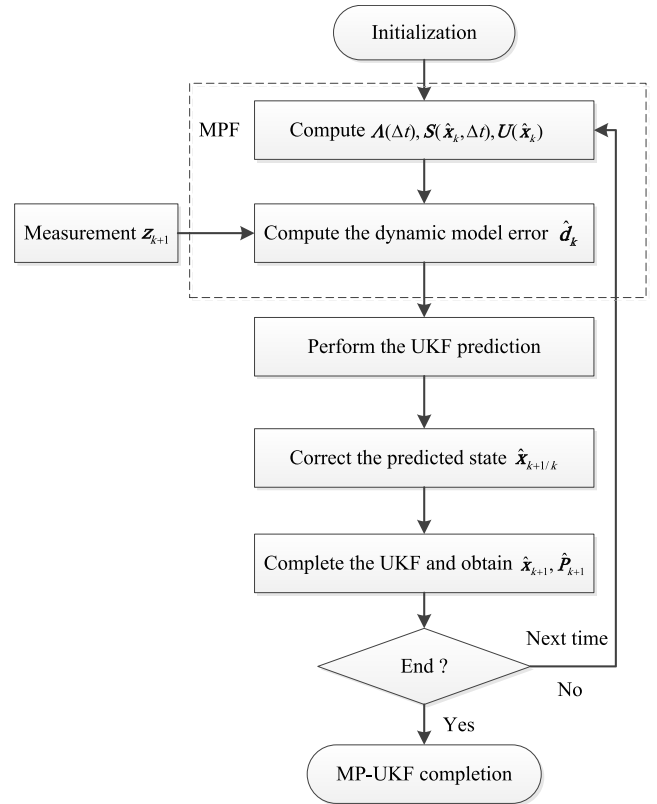

FIGURE 1. The flowchart of the proposed model predictive based unscented Kalman filter.

which is given by

$$\hat{x}_{k+1/k} = \sum_{i=0}^{2n} \omega_i f(\chi_{i,k}) + \Delta t \cdot \hat{d}_k \tag{35}$$

Step 4: Complete the UKF procedure according to (16)-(22) to obtain the system state estimation $\hat{x}_{k+1}$ and the corresponding error covariance matrix $\hat{P}_{k+1}$.

Step 5: Repeat Steps 1 to 4 for the next time step until all samples are processed.

IV. SIMULATION ANALYSIS AND DISCUSSION

Simulations have been conducted to comprehensively evaluate the performance of the proposed MP-UKF for hypersonic vehicle navigation with INS/GNSS integration. The comparison of MP-UKF with the classical UKF and AFUKF in [20] is also discussed in case of the typical dynamic model errors, i.e. the unknown bias and the perturbed Gaussian distribution.

As shown in Fig. 2, a dynamic flight trajectory is simulated according to the actual hypersonic vehicles, which involves various maneuvers such as climbing, pitching, rolling and turning. The initial position of the hypersonic vehicle was at north latitude 34.246°, east longitude 109.022° and altitude 40*km*. The initial velocities along the three axis of the E-N-U navigation frame were 0*m/s*, 2000*m/s* and 0*m/s*, respectively. The initial position error was (15m, 15m, 20m), initial velocity error (0.5m/s, 0.5m/s, 0.5m/s) and initial
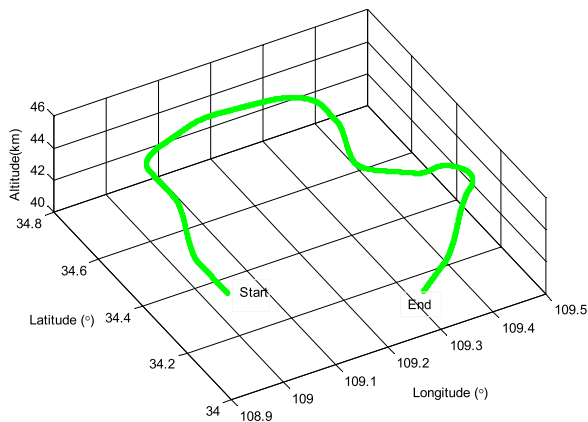
FIGURE 2. Flight trajectory of a hypersonic vehicle.

FIGURE 3. RMSE of the overall attitude error for hypersonic vehicle navigation with unknown bias case.

attitude error ($1'$, $1'$, $1.5'$). The gyro's constant drift and white noise were $0.1°$/h and $0.01°$/h. The accelerometer's zero bias and white noise were $10^{-3}g$ and $10^{-4}g$. The root mean square errors (RMSEs) of GNSS horizontal position, altitude and velocity were $5m$, $8m$ and $0.05m/s$. The sampling periods of INS and GNSS were 0.02s and 0.1s. The simulation time was 1000s and the filtering period of the INS/GNSS integration was 0.1s.

For the performance evaluation of the proposed MP-UKF in terms of dynamic model errors, two different cases are studied in the simulation analysis, which are as follows.

Case 1 (Unknown Bias Case): There exists unknown model bias in the dynamic model of INS/GNSS integration for hypersonic vehicle navigation. In the simulation, the model bias is assumed as a constant error as follow

$$\Delta \boldsymbol{x} = [\boldsymbol{0}_{1\times 3}, \ 0.05\text{m/s}, \ 0.05 \text{ m/s}, \ 0.05\text{m/s},$$
$$(3\times 10^{-6})', \ (3\times 10^{-6})', \ 10m, \ \boldsymbol{0}_{1\times 6}]^{\text{T}} \quad (36)$$

The above constant dynamic model error is introduced into the dynamic model of INS/GNSS integration during the time interval from 400s to 600s. Thus the dynamic model of INS/GNSS integration used for the Case 1 can be described as

$$\begin{cases} \boldsymbol{x}_k = f(\boldsymbol{x}_k) + \boldsymbol{w}_k, & \text{other time intervals} \\ \boldsymbol{x}_k = f(\boldsymbol{x}_k) + \Delta \boldsymbol{x} + \boldsymbol{w}_k, & (400s, 600s) \end{cases} \quad (37)$$

Case 2 (Perturbed Gaussian Distribution Case): The nominal Gaussian distribution of the process noise is perturbed by another distribution, i.e., the actual probability density function is

$$\rho_{actual} = (1-\varepsilon)\rho_{nominal} + \varepsilon\rho_{perturbing} \quad (38)$$

where ε is the ratio of the perturbing distribution, which is chosen as $0 < \varepsilon \le 0.5$. This distribution is called the contaminated Gaussian distribution. If $\rho_{perturbing}$ is also a Gaussian noise but with a larger standard deviation, the actual distribution ρ_{actual} is termed as a Gaussian mixture. In this study, the perturbing distribution is assumed to
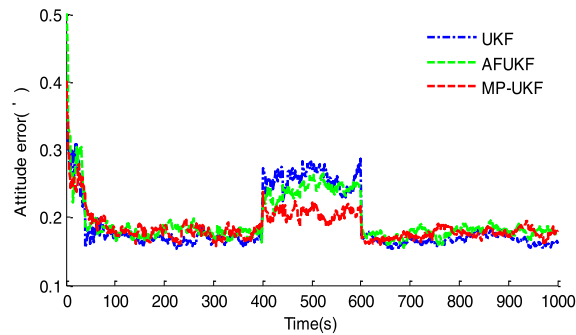
be Gaussian and its standard deviation is 10 times that of the nominal distribution. The ratio ε is set with the value of 0.3.

Monte Carlo simulations were conducted for 100 times at the same conditions to evaluate the navigation performance of MP-UKF in comparison with UKF and AFUKF. The root mean squared errors (RMSE) of the overall attitude error, overall velocity error and overall position error are computed to show the navigation performance of these methods from a statistical perspective. The RMSE is defined as

$$RMSE_k = \sqrt{\frac{1}{M}\sum_{i=1}^{M}(\hat{\boldsymbol{x}}_i - \boldsymbol{x}_{true})} \quad (39)$$

where M is the Monte Carlo runs.

The overall estimation error is defined as the norm of the navigation parameters estimation error, i.e.

$$\|\Delta\hat{x}\| = \sqrt{\Delta\hat{x}_E^2 + \Delta\hat{x}_N^2 + \Delta\hat{x}_U^2} \quad (40)$$

where $\Delta\hat{x}_E$, $\Delta\hat{x}_N$ and $\Delta\hat{x}_U$ are the components of $\Delta\hat{x}$ in East, North and Up, respectively.

Figs. 3-5 describe the RMSEs of the overall attitude errors, velocity errors and position errors by the UKF, AFUKF and proposed MP-UKF for Case 1. During the time intervals (400s, 600s), due to the influence of the introduced unknown model bias, the performance of UKF degrades seriously. This is because this method has no ability to resist the dynamic model error. The obtained RMSEs in attitude, velocity and position for the hypersonic vehicle are around $0.2578'$, 0.2132m/s and 17.9680m. The AFUKF weakens the influence of the unknown model bias on the filtering solution and improves the estimation accuracy of UKF, leading to the RMSEs in attitude, velocity and position around $0.2410'$, 0.1949m/s and 16.8439m. However, this method still has obvious estimation error since the adaptive fading factor in the AFUKF are determined by empiricism. As expected, because of the effective prediction of the involved dynamic model bias, the proposed MP-UKF achieves higher navigation accuracy than UKF and AFUKF in this time interval. Its estimated RMSEs in attitude, velocity and position for the hypersonic vehicle are around $0.2065'$, 0.1662m/s and
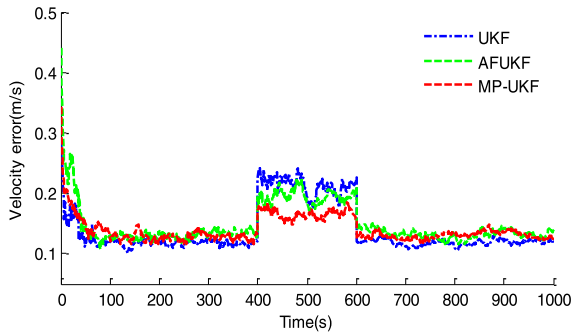
FIGURE 4. RMSE of the overall velocity error for hypersonic vehicle navigation with unknown bias case.
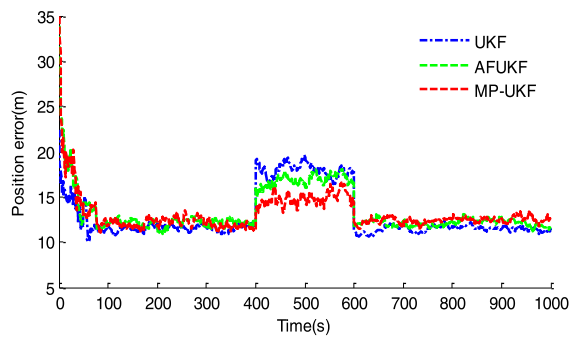

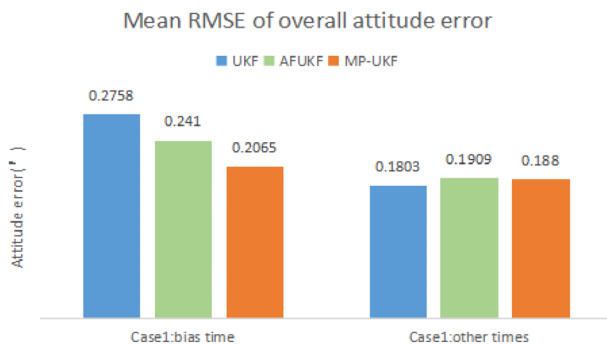**FIGURE 5.** RMSE of the overall position error for hypersonic vehicle navigation with unknown bias case.

FIGURE 6. Mean RMSE of the overall attitude error for hypersonic vehicle navigation with unknown bias case.

FIGURE 7. Mean RMSE of the overall velocity error for hypersonic vehicle navigation with unknown bias case.

FIGURE 8. Mean RMSE of the overall position error for hypersonic vehicle navigation with unknown bias case.

FIGURE 9. RMSE of the overall attitude error for hypersonic vehicle navigation with perturbed Gaussian distribution case.

14.8034m, respectively. Moreover, during the time intervals (0s, 400s) and (600s, 1000s), the estimation accuracy of the AFUKF and proposed MP-UKF is slightly lower than UKF. This is because the AFUKF and proposed MP-UKF are both the suboptimal filter, while the UKF can achieve the optimal estimation results in the absence of dynamic model errors. The estimated RMSEs in attitude, velocity and position for the hypersonic vehicle are around $0.1803'$, 0.1236m/s and 11.9531m for UKF; $0.1909'$, 0.1421m/s and 12.9930m for AFUKF; and $0.1880'$, 0.1364m/s and 12.9919m for the proposed MP-UKF, respectively.

Figs. 6-8 depict the intuitive comparison of the UKF, AFUKF and proposed MP-UKF for the mean RMSEs of the overall attitude errors, velocity errors and position
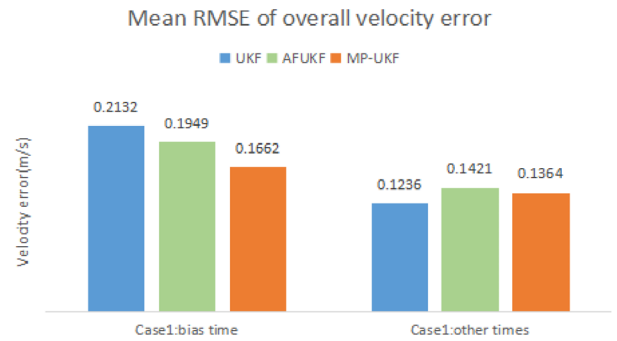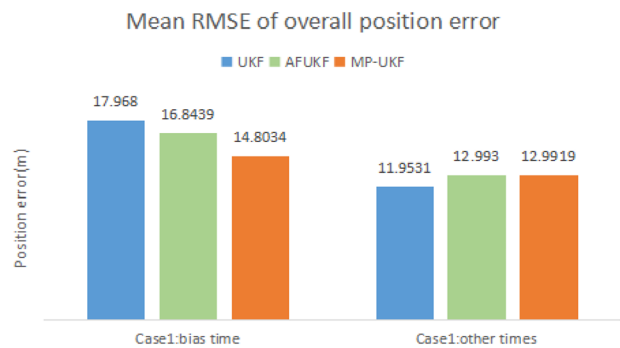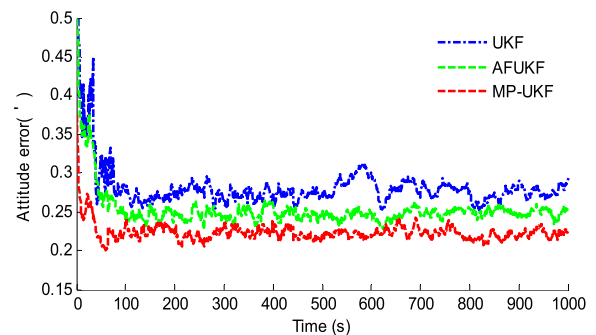
errors for Case 1. These also verify that the proposed MP-UKF has a stronger ability to resist the unknown dynamic model bias, thus leading to improved navigation accuracy for the hypersonic vehicle navigation with INS/GNSS integration.

Figs. 9-11 show the RMSEs of the overall attitude errors, velocity errors and position errors of the hypersonic vehicle by the UKF, AFUKF and proposed MP-UKF for Case 2. From Figs. 9-11, it can be seen that as the process noise distribution is perturbed, the navigation accuracy of UKF is the lowest among the above three filters, leading to the RMSEs in attitude, velocity and position around $0.2818'$, 0.2104m/s and 18.1226m, respectively. The accuracy of AFUKF is relatively superior to that of UKF due to the
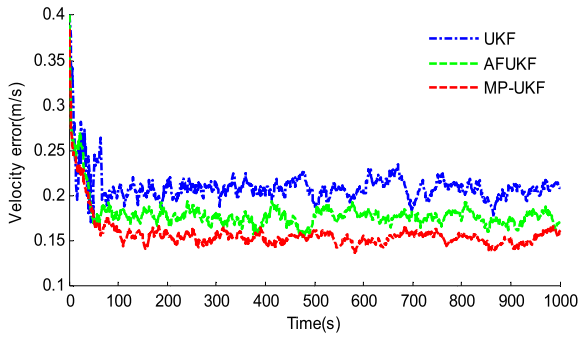
FIGURE 10. RMSE of the overall velocity error for hypersonic vehicle navigation with perturbed Gaussian distribution case.
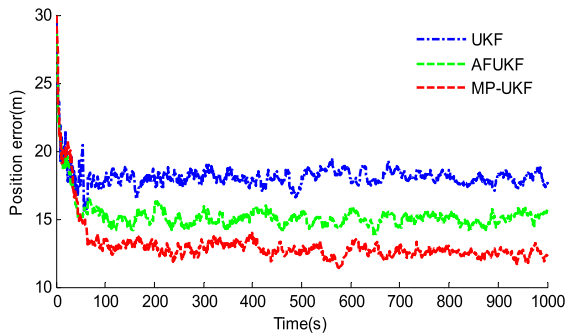

FIGURE 11. RMSE of the overall position error for hypersonic vehicle navigation with perturbed Gaussian distribution case.
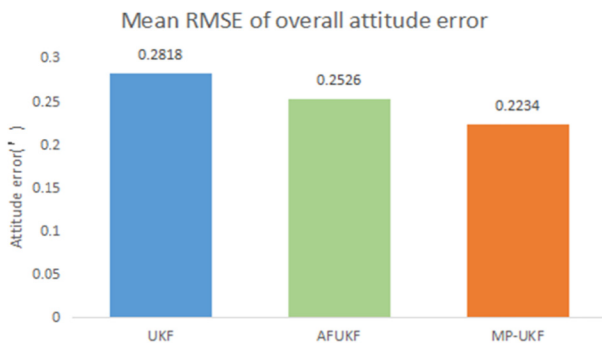

FIGURE 12. Mean RMSE of the overall attitude error for hypersonic vehicle navigation with perturbed Gaussian distribution case.

FIGURE 13. Mean RMSE of the overall velocity error for hypersonic vehicle navigation with perturbed Gaussian distribution case.

FIGURE 14. Mean RMSE of the overall position error for hypersonic vehicle navigation with perturbed Gaussian distribution case.

ability to resist the perturbed Gaussian noise. The obtained RMSEs in attitude, velocity and position of the hypersonic vehicle are around $0.2526'$, 0.1801m/s and 15.2279m. Not surprisingly, the proposed MP-UKF has higher navigation accuracy than the AFUKF in which the adaptive fading factor is empirically determined. The RMSEs in attitude, velocity and position of the hypersonic vehicle for the proposed MP-UKF are around $0.2234'$, 0.1581m/s and 13.0926m. Figs. 12-14 also depict the intuitive comparison of the UKF, AFUKF and proposed MP-UKF about the mean RMSEs of the overall attitude errors, velocity errors and position errors with the perturbed Gaussian distribution case. These results confirm the above mentioned conclusions as well.
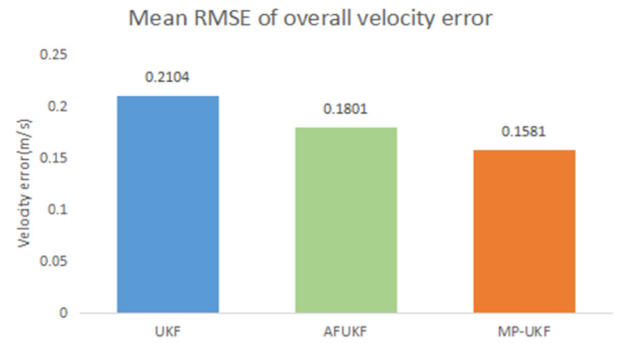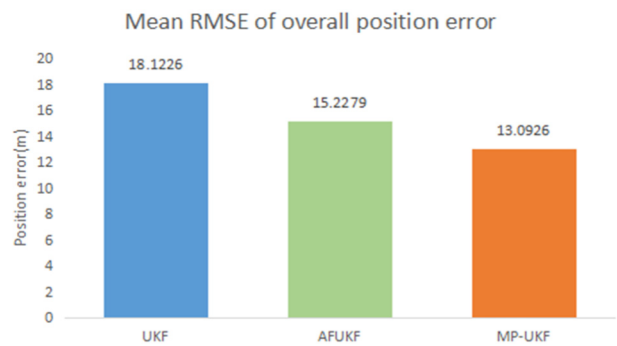
The above simulations and analysis conclude that the proposed MP-UKF can restrain the effect of the dynamic model errors on the navigation solution effectively, leading to smaller navigation errors than UKF and AFUKF for the hypersonic vehicle navigation with INS/GNSS integrated system.

V. CONCLUSION

This paper proposes a new MP-UKF for hypersonic vehicle navigation with INS/GNSS integration to address the performance degradation due to the dynamic model errors involved. The MP-UKF employs the concept of MPF to improve the UKF adaptiveness and furtherly resist the effect of dynamic model error on navigation solution. It corrects the UKF sensitivity to dynamic model error in the filtering procedure through the estimation and compensation of the error online. Thus the MP-UKF overcomes the limitation of UKF and is promising to provide reliable filtering results for systems in presence of dynamic model error. The simulation results and comparison analysis have demonstrated that the proposed MP-UKF has preferable estimation accuracy than UKF and AFUKF for INS/GNSS integration in hypersonic vehicle navigation.

Future research work will focus on the improvement of the proposed MP-UKF. It is expected to combine the proposed MP-UKF with artificial intelligence technologies such as pattern recognition, neural network and advanced

expert systems to automatically identify the dynamic model errors.

REFERENCES

[1] C. Bahm, E. Baumann, J. Martin, D. Bose, R. Beck, and B. Strovers, "The X–43A hyper–X mach 7 flight 2 guidance, navigation, and control overview and flight test results," in *Proc. AIAA/CIRA 13th Int. Space Planes Hypersonics Syst. Technol. Conf.*, Capua, Italy, May 2005, p. 3275.

[2] H. L. Besser, D. Göge, M. Huggins, A. Shaffer, and D. Zimper, "Hypersonic vehicles-game changers for future warfare?" *Transf. Joint Air Power, J. JAPCC*, vol. 24, pp. 11–27, Jul. 2017.

[3] P. Ouzts, D. Soloway, D. Moerder, D. Wolpert, and J. Benavides, "The role of guidance, navigation, and control in hypersonic vehicle multidisciplinary design and optimization," in *Proc. 16th AIAA/DLR/DGLR Int. Space Planes Hypersonics Syst. Technol. Conf.*, Bremen, Germany, Oct. 2009, p. 7329.

[4] M. Samaan and S. Theil, "Development of a low cost star tracker for the SHEFEX mission," *Aerosp. Sci. Technol.*, vol. 23, no. 1, pp. 469–478, Dec. 2012.

[5] G. Hu, B. Gao, Y. Zhong, L. Ni, and C. Gu, "Robust unscented Kalman filtering with measurement error detection for tightly coupled INS/GNSS integration in hypersonic vehicle navigation," *IEEE Access*, vol. 7, pp. 151409–151421, 2019.

[6] R. Wang, Z. Xiong, J. Liu, J. Xu, and L. Shi, "Chi-square and SPRT combined fault detection for multisensor navigation," *IEEE Trans. Aerosp. Electron. Syst.*, vol. 52, no. 3, pp. 1352–1365, Jun. 2016.

[7] G. Hu, S. Gao, and Y. Zhong, "A derivative UKF for tightly coupled INS/GPS integrated navigation," *ISA Trans.*, vol. 56, pp. 135–144, May 2015.

[8] J. Crassidis, "Sigma-point Kalman filtering for integrated GPS and inertial navigation," *IEEE Trans. Aerosp. Electron. Syst.*, vol. 42, no. 2, pp. 750–756, Apr. 2006.

[9] K. Chen, "Strapdown inertial navigation algorithm for hypersonic boost–glide vehicle," in *Proc. 21st AIAA Int. Space Planes Hypersonics Technol. Conf.*, Xiamen, China, Mar. 2017, p. 2174.

[10] G. Hu, W. Wang, Y. Zhong, B. Gao, and C. Gu, "A new direct filtering approach to INS/GNSS integration," *Aerosp. Sci. Technol.*, vol. 77, pp. 755–764, Jun. 2018.

[11] H. Carvalho, P. Del Moral, A. Monin, and G. Salut, "Optimal nonlinear filtering in GPS/INS integration," *IEEE Trans. Aerosp. Electron. Syst.*, vol. 33, no. 3, pp. 835–850, Jul. 1997.

[12] B. Cui, X. Chen, Y. Xu, H. Huang, and X. Liu, "Performance analysis of improved iterated cubature Kalman filter and its application to GNSS/INS," *ISA Trans.*, vol. 66, pp. 460–468, Jan. 2017.

[13] M.-J. Yu, "INS/GPS integration system using adaptive filter for estimating measurement noise variance," *IEEE Trans. Aerosp. Electron. Syst.*, vol. 48, no. 2, pp. 1786–1792, Apr. 2012.

[14] S. Gao, G. Hu, and Y. Zhong, "Windowing and random weighting-based adaptive unscented Kalman filter," *Int. J. Adapt. Control Signal Process.*, vol. 29, no. 2, pp. 201–223, Feb. 2015.

[15] G.-G. Hu, S.-S. Gao, Y.-M. Zhong, and B.-B. Gao, "Stochastic stability of the derivative unscented Kalman filter," *Chin. Phys. B*, vol. 24, no. 7, Jul. 2015, Art. no. 070202.

[16] H. M. T. Menegaz, J. Y. Ishihara, G. A. Borges, and A. N. Vargas, "A systematization of the unscented Kalman filter theory," *IEEE Trans. Autom. Control*, vol. 60, no. 10, pp. 2583–2598, Oct. 2015.

[17] G. Hu, S. Gao, Y. Zhong, B. Gao, and A. Subic, "Modified strong tracking unscented Kalman filter for nonlinear state estimation with process model uncertainty," *Int. J. Adapt. Control Signal Process.*, vol. 29, no. 12, pp. 1561–1577, Dec. 2015.

[18] B. Xu, S. Wang, D. Gao, Y. Zhang, and Z. Shi, "Command filter based robust nonlinear control of hypersonic aircraft with magnitude constraints on states and actuators," *J. Intell. Robot. Syst.*, vol. 73, nos. 1–4, pp. 233–247, Jan. 2014.

[19] V. Karachun, V. Mel'nick, I. Korobiichuk, M. Nowicki, R. Szewczyk, and S. Kobzar, "The additional error of inertial sensors induced by hypersonic flight conditions," *Sensors*, vol. 16, no. 3, p. 299, Feb. 2016.

[20] H. E. Soken and C. Hajiyev, "Adaptive fading UKF with Q–adaptation: Application to picosatellite attitude estimation," *J. Aerosp. Eng.*, vol. 26, no. 3, pp. 628–636, Jul. 2013.

[21] S. Cho and W. Choi, "Robust positioning technique in low–cost DR/GPS for land navigation," *IEEE Trans. Instrum. Meas.*, vol. 55, no. 4, pp. 1132–1142, Aug. 2006.

[22] Y. Meng, S. Gao, Y. Zhong, G. Hu, and A. Subic, "Covariance matching based adaptive unscented Kalman filter for direct filtering in INS/GNSS integration," *Acta Astronaut.*, vol. 120, pp. 171–181, Mar. 2016.

[23] Q. Song, "An adaptive UKF algorithm for the state algorithm for the state and parameter estimations of a mobile robot," *Acta Automat. Sinica*, vol. 34, no. 1, pp. 72–79, May 2008.

[24] J. L. Crassidis and F. L. Markley, "Predictive filtering for nonlinear systems," *J. Guid., Control, Dyn.*, vol. 20, no. 3, pp. 566–572, 1997.

[25] J. L. Crassidis and F. L. Markley, "Predictive filtering for attitude estimation without rate sensors," *J. Guid., Control, Dyn.*, vol. 20, no. 3, pp. 522–527, May 1997.

[26] J. Fang and X. Gong, "Predictive iterated Kalman filter for INS/GPS integration and its application to SAR motion compensation," *IEEE Trans. Instrum. Meas.*, vol. 59, no. 4, pp. 909–915, Apr. 2010.

[27] B. Q. Liu, X. L. Gong, and J. C. Fang, "In-flight self-alignment for airborne SINS/GPS based on GPS observation and model predict filter," *J. Chin. Inertial Technol.*, vol. 15, no. 5, pp. 568–572, 2007.

[28] K. Xiong, L. Liu, and H. Zhang, "Modified unscented Kalman filtering and its application in autonomous satellite navigation," *Aerosp. Sci. Technol.*, vol. 13, nos. 4–5, pp. 238–246, Jun. 2009.

GAOGE HU received the B.S. degree in mathematics and applied mathematics from Northwest Polytechnical University, Xi'an, China, in 2010, and the Ph.D. degree in control theory and control engineering from Northwest Polytechnical University, in 2016. From 2016 to 2017, he worked as a System Engineer with the Huawei Technologies Company, Ltd. He is currently an Associate Professor with the School of Automation, Northwest Polytechnical University. His current research interests include integrated navigation, Kalman filtering, nonlinear state estimation, and multisensors data fusion.
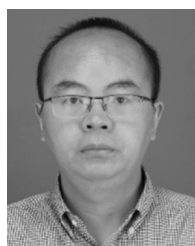
LONGQIANG NI received the M.S. and Ph.D. degrees in traffic information engineering and control from Northwest Polytechnical University, Xian, China, in 2008 and 2016, respectively. From 2003 to 2005, he was an Assistant Engineer with SINOPEC Yanshan Petrochemical Company, Beijing, China. In 2008, he was an Engineer with the Northwestern Institute of Mechanical and Engineering, Xianyang, China, where he is currently an Associate Research Fellow. His research interests are navigation, control and decision making, nonlinear control, and sensor networks.

BINGBING GAO received the Ph.D. degree in navigation, guidance, and control from Northwest Polytechnical University, Xian, China, in 2018. He is currently an Assistant Professor with the School of Automation, Northwest Polytechnical University. His research interests include information fusion, nonlinear filtering, and integrated navigation.
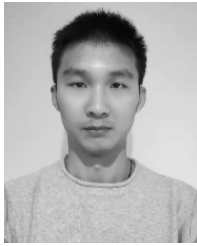
XINHE ZHU received the B.S. degree (Hons.) in aerospace and aviation engineering from RMIT University, Melbourne, VIC, Australia, in 2017, where he is currently pursuing the Ph.D. degree with the School of Aerospace, Mechanical and Manufacturing Engineering. His research interests are robotics control, soft tissue modeling, surgical simulation, aerospace navigation and control, nonlinear filter, and haptics control.

YONGMIN ZHONG is currently an Associate Professor with the School of Aerospace, Mechanical and Manufacturing Engineering, RMIT University, Australia. His research interests include computational engineering, haptics, soft tissue modeling, surgical simulation, aerospace navigation and control, intelligent systems, and robotics.

• • •

WEI WANG received the Ph.D. degree in traffic information engineering and control from Northwest Polytechnical University, Xi'an, China, in 2019. He is currently serving as an Engineer with CRRC Yongji Electric Company, Xi'an. His research interests are motor control, navigation, and sensor networks.